

# Formation of shear-bands in drying colloidal dispersions

Pree-Cha Kiatkirakajorn<sup>1</sup> and Lucas Goehring<sup>1,\*</sup>

<sup>1</sup>Max Planck Institute for Dynamics and Self-Organization (MPIDS), 37077 Göttingen, Germany

(Dated: May 18, 2022)

In directionally-dried colloidal dispersions regular bands can appear behind the drying front, inclined at  $\pm 45^\circ$  to the drying line. These have been described as shear bands, based on similarities to such features in metals. Through microscopy of silica and polystyrene dispersions, dried in Hele-Shaw cells, we confirm that the bands are associated with local shear strains. We further show how the bands form, that they scale with the thickness of the drying layer, and demonstrate that they are eliminated by the addition of salt to the drying dispersions. Finally, we reveal the origins of these bands in the compressive forces associated with drying, and show how they affect the optical properties (birefringence) of colloidal films and coatings.

Colloidal dispersions are the basis of many paints, inks and coatings, are used in ceramics and composites, and are a basis of the photonics industry. When dried, these dispersions can show a surprising variety of patterning mechanisms. They may buckle [1], or crack into spirals [2], waves [3], or parallel lines [4], for example, while their dried shape can vary from a coffee-ring [5] to textured surfaces controlled by evaporation-lithography [6, 7]. This abundance of patterns, recently reviewed in [8, 9], suggests diverse means for the directed self-assembly of micro-structured materials, if the underlying dynamics can be understood and controlled. In this letter we look at a pattern of angled bands that commonly appears in drying dispersions (see Fig. 1) and confirm by direct means that they are, indeed, shear bands. We then show how the pattern scales, how it can be suppressed, and discuss its origins in the compressive forces that accompany the directional drying of colloidal dispersions.

Shear bands in dried sol-gels were first seen by Hull and Caddock [10], who studied desiccation as an analog for thermal contraction in geophysical settings. For colloidal silica (Ludox TM-50) they found that regular bands always preceded fracture. These bands were oriented at  $\pm 45^\circ$  to the cracks and identified as shear bands, based on their appearance. Berteloot *et al.* then described identical bands on the surface of drying droplets of colloidal silica (Klebosol) [11]. They were suggested to be either shear bands, based on a visual similarity to such features in metals [12], or the surface buckling of a colloidal skin. Boulogne *et al.* also noted regular bands when colloidal silica (Ludox HS) is dried in Hele-Shaw cells, and argued how they could be driven by plastic yielding during solidification [13]. Finally, Yang *et al.* have recently shown that in polystyrene dispersions the width of bands – *i.e.* the fraction of sheared material – scales with the shear rate of drying as expected for a plastic deformation [14].

To prepare banded films, we used a variety of charge-stabilized colloidal dispersions. Polystyrene dispersions with particle diameters  $d$  of 98, 100, 105, 115, 144, 198 and 283 nm were synthesized as described elsewhere [15]. Colloidal silica was used for additional observations: Lu-

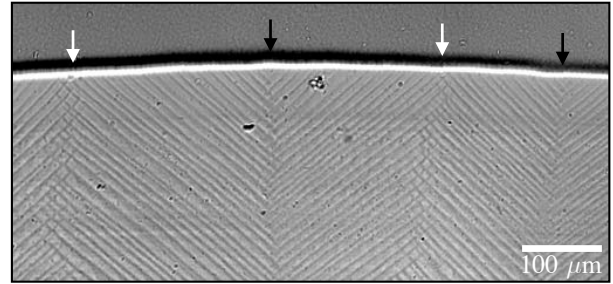


FIG. 1. Drying colloidal polystyrene in a free-standing film. The drying front is a bright horizontal line, with liquid film above it, and solid film below. The shear bands in the solid are angled away from the drying front. Domains of left-leaning and right-leaning bands can meet in two ways: junctions that open towards the drying front (black arrows) are sources of new bands, while these that open away from the front (white arrows) are where growing bands end.

dox HS (Sigma-Aldrich,  $d = 16$  nm) was dialyzed against aqueous solutions of 5 mM NaCl at pH 9.5 (by addition of NaOH); Levasil-30 (Azko-Nobel,  $d = 92$  nm [13]) was used as received. NaCl solutions were then mixed with the above materials to form dispersions of  $\sim 5\%$  solids by volume, and salt concentrations of up to 60 mM. Deionized water (Millipore) was used for all procedures.

Drying experiments were performed in Hele-Shaw cells built from two  $2.5 \times 7.5$  cm glass microscope slides, as in Fig. 2. Interposed between the slides, along their long edges, were plastic spacers of either 150, 230, 250, 300, 400 or 500  $\mu\text{m}$ . The cells were held together by reusable clips and the actual cell thicknesses  $h$  were measured by microscopy after assembly. Thinner cells, with  $h$  between 36–72  $\mu\text{m}$ , were made with heat-curable polymer sheets or double-sided tape (50  $\mu\text{m}$ ) as spacers. In each experiment a dispersion was pipetted into the cavity of a cell. The sample then dried by evaporation from one of the open short edges of the cell, at room temperature. During drying the cell was inclined by a few millimeters, so that any bubbles rose away from the drying edge by buoyancy.

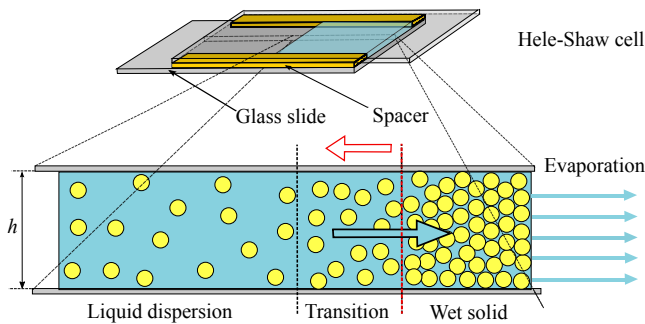


FIG. 2. Drying cells were made in a Hele-Shaw geometry. A dispersion was drawn into a cell and then dried naturally from one edge. As drying proceeded, a solid region slowly grew into the still-liquid dispersion. On close inspection the solidification front is a narrow transition region that contains strong gradients in particle concentration, over which the dispersion’s properties rapidly change.

The drying of these dispersions proceeds by the advance of a solidification front into the colloidal liquid (see *e.g.* [4, 8, 16, 17]), as sketched in Fig. 2. The solid film remains porous and water flows through it to balance evaporation from its open edge. This flow continuously brings more colloidal particles with it, which add to the growing solid deposit. The viscous drag of the water, flowing past these particles, is balanced by a gradient in their osmotic pressure, and hence a concentration gradient forms in the liquid leading up to the solidification front. Along this gradient the character of the dispersion can change rapidly, and dramatically. For example, in charge-stabilized dispersions, as we use here, the particles may first be concentrated into a soft repulsive solid, where each particle is caged by long-range electrostatic interactions with its neighbors [17]. The drag from the flow through this soft solid is equivalent to a uniaxial compression and can cause effects like structural anisotropy and birefringence [13]. Eventually the particles are pushed close enough together for short-range van der Waals forces to overcome their electrostatic repulsion. At this point the particles will jump into intimate contact, forming into an attractive, rigid film [17].

We found shear bands in our dried colloidal films, in both Hele-Shaw geometries and in free-standing droplets dried from the same materials. Generally, as shown in Fig. 1, or in the supplemental movie [18], the bands appeared as a dispersion changed from a liquid to a solid. They arranged into domains of stripes inclined to either the left or the right of the drying front. These domains overlapped by about one wavelength of the banding, to form domain boundaries that looked like chevrons [14] opening either towards the drying front, or away from it.

The chevrons that opened towards the drying front periodically generated new bands, which appeared alternately to one side of the chevron, and then to the other. The chevrons that opened away from the drying front

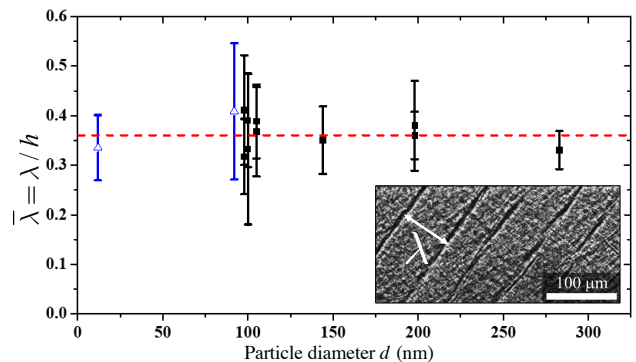


FIG. 3. The relative band spacing  $\bar{\lambda}$  was measured in 150  $\mu\text{m}$  thick cells. For colloidal latex (solid black) and silica (open blue) at low ionic strength (1-5  $\mu\text{M}$ ), there is no dependence of the relative spacing on particle size. Bars show the standard deviation of each measurement.

were sinks for growing bands. New bands could also appear between two existing bands, if they were far enough apart. A new band typically began at a point and generated two ‘tips’ that propagated simultaneously towards and away from the drying front, over several seconds. Banding always occurred well before any cracks opened.

The shear bands approached the liquid-solid boundary at an angle of  $45^\circ$ , but the bands were compressed along the direction of drying, over time. This smooth bending of the bands can be seen near the solid-liquid transition of Fig. 1, or in the supplemental movie [18]. Later, if a film cracked, the bands were also compressed by the crack opening. Looking at 21 different films, in both free-standing and Hele-Shaw geometries, we found that the final opening angle of the chevrons was  $99 \pm 7^\circ$  (mean  $\pm$  standard deviation) in fully dried films. There was no clear dependence on particle size or film thickness.

The most obvious feature of the bands is their relatively even spacing,  $\lambda$ . We observed fully dried bands in a range of colloidal materials, and a variety of conditions. For each of eight different sizes of colloidal silica and polystyrene we prepared 150  $\mu\text{m}$  thick Hele-Shaw cells, filled with 180  $\mu\text{l}$  of dispersion. Once dry, we imaged these cells by digital microscopy under transmitted light. We scanned across the width of each cell, collected images in about ten different locations, and measured about 20 band spacings (measured normal to the bands) per image.

Figure 3 shows that there was no dependence of the band spacing on the particle size, for particles between 16 and 283 nm. The bands were, on average, 0.36 times the film thickness  $h$ . An equal mixture of two particle sizes, 98 and 198 nm, was also consistent ( $\lambda/h = 0.29 \pm 0.13$ ) with this result. However, although the bands are parallel and have a clearly defined spacing, there can be a wide variation in this spacing within a single cell: as in Fig. 1, patches of wider or narrower bands often appear together, with no apparent reason for the local variation in size.

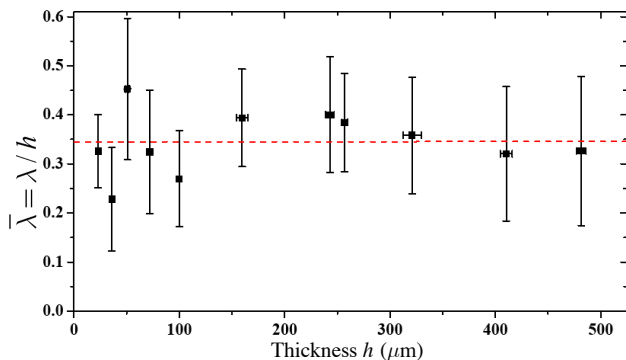


FIG. 4. The relative band spacing was measured in cells of different thicknesses, using dispersions with about 100 nm particles. There is no dependence of  $\bar{\lambda}$  on  $h$ ; the band spacing is simply proportional to the thickness of the drying layer.

As such, we report the standard deviation (rather than the standard error) of our measurements, throughout this letter. Bands regularly appeared with a range of spacings from 0.2 to 0.5 times the film thickness.

Dispersions with  $d \simeq 100$  nm (each experiment was repeated with 92 nm silica and 105 and 115 nm polystyrene particles) were then dried in cells of different thicknesses. Figure 4 shows that there was no dependence of the relative band spacing  $\bar{\lambda} = \lambda/h$  on the thickness of the drying film. In other words, the band spacing scales linearly with  $h$ . Although there was, again, considerable variation within the results, the average  $\bar{\lambda} = 0.34$  is in agreement with the results for changing particle size (Fig. 3).

Finally, we studied how the formation of bands was influenced by the salinity of the initial dispersions. For charged colloidal particles, dissolved salt screens electrostatic interactions, affecting the cooperative behavior of the particles. We therefore dried 105 and 198 nm colloidal polystyrene and 16 nm colloidal silica in NaCl solutions of up to 60 mM, in 150  $\mu\text{m}$  thick cells. Figure 5 shows that for each particular dispersion there is a cut-off salt concentration above which bands do not form. This critical concentration depends on particle size and particle type. Below the critical concentration there also appears to be a weak dependence of the band spacing on salt: the bands are closer together in saltier dispersions. Otherwise, however, all these dispersions dried exactly as before, *via* directional solidification, and cracked cleanly.

These experiments collectively suggest how bands form by an elastic instability, similar to fracture. They are Mode-II (sliding) cracks, or shear bands, that act to release the shear stresses that accompany directional solidification, just as the opening cracks that often form in drying paints relax in-plane tensions.

Cracks in a thin elastic film are usually regularly spaced by a small multiple of the film thickness [4, 19]. This follows from how they release strain energy. For example, the height-averaged strains near a straight crack

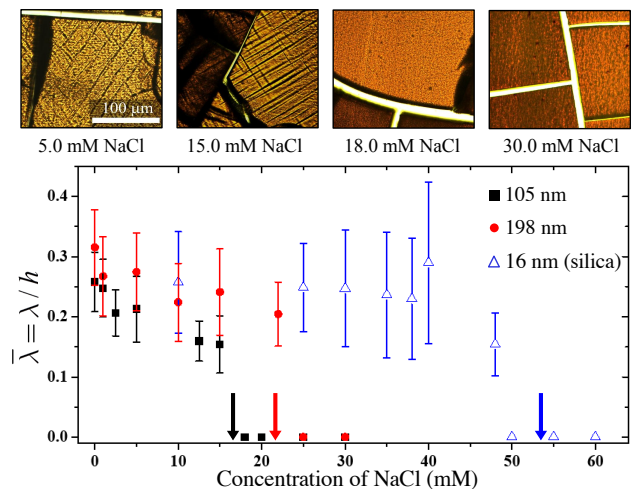


FIG. 5. Shear bands may be eliminated ( $\bar{\lambda} = 0$  indicates no banding) by the addition of salt, with a critical level depending on particle size and composition. Arrows mark where the strongest interactions between neighboring particles (Eq. 1) drop below  $5kT$ . Above, images show how the bands change with salt concentration, for 105 nm polystyrene.

in a thin film, with a rigid boundary, decay away over a distance proportional to  $h$  [20]. The same mechanics requires that distortions rapidly decay away from a shear band, in a film attached to rigid walls, and that the mature band spacing should be proportional to the film thickness, as we have shown it is.

During drying, the colloidal dispersion is subjected to a uniaxial compression, caused by the drag of water flowing past the particles to the evaporating edge. Under these conditions the direction of maximum shear stress is at  $\pm 45^\circ$  to the direction of compression: for principle stresses  $\sigma_1$  and  $\sigma_2$  the shear stress at an orientation  $\theta$  to the compression axis is  $((\sigma_2 - \sigma_1)/2) \sin(2\theta)$ . The von Mises yield criterion (see *e.g.* [21]) states that plastic failure is expected when the magnitude of this stress exceeds some critical value, and that failure will occur along the direction of maximum shear stress. Thus the orientation of the bands, and the position of their formation, shows that they relieve the shear stresses generated near the solidification front. The shear motion around the bands themselves can be seen directly in cases where bands overlap significantly, as in Fig. 6(a). Later deformation, including cracking, will distort the inclination of the shear bands, but is not related to their formation.

Directionally dried colloidal films are birefringent, as their entire structure is compressed along the direction of drying [13, 22]. The birefringence around the shear bands, as shown in Fig. 6(b), is a measure of how the bands bend the film around them. The optical axis of a material is a direction along which birefringent effects vanish. We positioned our films in a cross-polarizing microscope equipped with a first-order retardation plate,

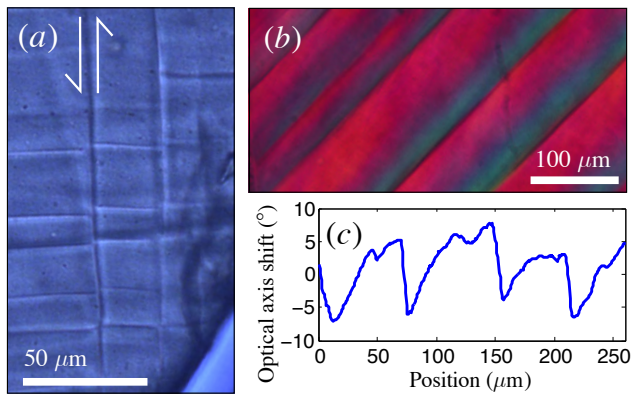


FIG. 6. Shear deformation. (a) A later band will displace any earlier bands to either side of it like a fault. (b) Dry films are birefringent. Under cross-polarized light a homogenous film should appear purple here. A clockwise rotation of the optical axis shifts the color towards blue, while the opposite motion shifts it to red. (c) The optical axis of a film (Levasil) shifts by  $\pm 5^\circ$  around the bands, showing how the entire bulk structure of the film is twisted by band formation.

so that the optical axis at a point half-way between the bands was aligned with the polarization of the transmitted light. We measured the optical axis shift at different points by finding the relative rotation required to minimize transmitted light of 546 nm. As shown in Fig. 6(c), the formation of a shear band twists the entire structure of the film, rotating the optical axis (*i.e.* the direction of maximum compression of the film) by  $\pm 5^\circ$  to either side of it. The sawtooth-pattern of the birefringence shows how slip is highly localized in the shear band, and how strains decay away smoothly from the slip plane.

Finally, we discuss the extinction of the shear bands with addition of salt, which shows why band formation is localized at the liquid-solid transition of directional drying. The DLVO model of colloidal stability combines an attractive van der Waals potential at short distances with a repulsive electrostatic interaction that is screened by ions in solution [23]. We use the pair potential

$$U = -\frac{Ad}{24s} + \frac{4dkT}{L_B} \tanh^2(\Phi)e^{-\kappa s} \quad (1)$$

to approximate the free energy of two neighboring particles of surface-separation  $s$ . Here,  $A$  is the Hamaker constant ( $5 \cdot 10^{-21}$  J for polystyrene [17], and  $8 \cdot 10^{-21}$  J for silica [23]),  $L_B = 0.7$  nm is the Bjerrum length,  $kT$  is the Boltzmann energy and  $\kappa^{-1}$  is the Debye length.  $\Phi$  is a reduced surface potential, calculated as in [17] with a surface charge density of  $0.53 \mu\text{C}/\text{cm}^2$  for polystyrene particles (measured in [17]), and  $2.5 \mu\text{C}/\text{cm}^2$  for silica (chosen to match the zeta potentials in [24]). Adding salt lowers both  $\kappa^{-1}$  and  $\Phi$ . Experience has shown that colloidal crystals [23] or glasses [13] will form when a

dispersion is concentrated to the point where the pair potential at an average particle separation reaches a few times  $kT$ . Above this threshold the repulsive forces between particles can give rise to effective cages, freezing particles into a semi-rigid arrangement.

For the three cases studied we find that the shear bands disappear at the salt concentrations where the maximum value of  $U(s)$  is lowered to  $5kT$  (arrows in Fig. 5). In other words, the bands vanish when the electrostatic interaction is weakened to the point that a soft repulsive solid does not have the opportunity to form during the transition from a colloidal liquid to an aggregated solid film. Since salt will not significantly affect the properties of the aggregated solid, this demonstrates that it is the compression across the liquid-solid transition itself that is responsible for shear band formation.

In this letter we have shown how the shear bands that regularly appear in dried colloidal films form and scale. The bands relieve the compressive stresses associated with directional drying, by localized slip at  $45^\circ$  to the axis of compression. In particular, we have shown how the bands are driven by the compression of a soft intermediate phase that can form around the liquid-solid transition, when particles are caged by their electrostatic interactions. By engineering the response of this transition region, such as by adding salt to weaken inter-particle forces, the bands can be controlled or eliminated.

We thank Anupam Sengupta and Carsten Krüger for assistance with the birefringence measurements, and Antoine Fourrière for helpful discussions. PK thanks the Thai DPST and Government of Thailand for funding.

\* lucas.goehring@ds.mpg.de

- [1] N. Tsapis, E. R. Dufresne, S. S. Sinha, C. S. Riera, J. W. Hutchinson, L. Mahadevan, and D. A. Weitz, *Phys. Rev. Lett.* **94**, 018302 (2005).
- [2] V. Lazarus and L. Pauchard, *Soft Matter* **7**, 2552 (2011).
- [3] L. Goehring, W. J. Clegg, and A. F. Routh, *Soft Matter* **7**, 7984 (2011).
- [4] C. Allain and L. Limat, *Phys. Rev. Lett.* **74**, 2981 (1995).
- [5] R. D. Deegan, O. Bakajin, T. F. Dupont, G. Huber, S. R. Nagel, and T. A. Witten, *Nature* **389**, 827 (1997).
- [6] D. J. Harris, H. Hu, J. C. Conrad, and J. A. Lewis, *Phys. Rev. Lett.* **98**, 148301 (2007).
- [7] C. Parneix, P. Vandoolaeghe, V. S. Nikolayev, D. Quéré, J. Li, and B. Cabane, *Phys. Rev. Lett.* **105**, 266103 (2010).
- [8] A. F. Routh, *Rep. Prog. Phys.* **76**, 046603 (2013).
- [9] U. Thiele, *Adv. Colloid Int. Sci.* **206**, 399 (2014).
- [10] D. Hull and B. Caddock, *J. Mat. Sci.* **34**, 5707 (1999).
- [11] G. Berteloot, A. Hoang, A. Daerr, H. P. Kavehpour, F. Lequeux, and L. Limat, *J. Colloid Interface Sci.* **370**, 155 (2012).
- [12] J. Schroers and W. L. Johnson, *Phys. Rev. Lett.* **93**, 255506 (2004).
- [13] F. Boulogne, L. Pauchard, F. Giorgiutti-Dauphiné,

- R. Botet, R. Schweins, M. Sztucki, J. Li, B. Cabane, and L. Goehring, *Europhys. Lett.* **105**, 38005 (2014).
- [14] B. Yang, J. S. Sharp, and M. Smith, *ACS Nano*, 10.1021/acs.nano.5b00127 (In press).
- [15] H. N. Yow, M. Goikoetxea, L. Goehring, and A. F. Routh, *J. Colloid Interface Sci.* **352**, 542 (2010).
- [16] E. R. Dufresne, E. I. Corwin, N. A. Greenblatt, J. Ashmore, D. Y. Wang, A. D. Dinsmore, J. X. Cheng, X. S. Xie, J. W. Hutchinson, and D. A. Weitz, *Phys. Rev. Lett.* **91**, 224501 (2003).
- [17] L. Goehring, W. J. Clegg, and A. F. Routh, *Langmuir* **26**, 9269 (2010).
- [18] See Supplemental Material at <https://youtu.be/vnI6WdmG6ug> for a movie of shear band formation.
- [19] T. Bai, D. D. Pollard, and H. Gao, *Nature* **403**, 753 (2000).
- [20] Z. C. Xia and J. W. Hutchinson, *J. Mech. Phys. Solids* **48**, 1107 (2000).
- [21] T. L. Anderson, *Fracture mechanics, fundamentals and applications*, 3rd ed. (Taylor & Francis, New York, 2000) p. 610.
- [22] K. Yamaguchi, S. Inasawa, and Y. Yamaguchi, *Phys. Chem. Chem. Phys.* **15**, 2897 (2013).
- [23] W. B. Russel, D. A. Saville, and W. R. Schowalter, *Colloidal dispersions* (Cambridge University Press, Cambridge, 1989) p. 525.
- [24] T. W. Healy, in *Colloidal Silica. Fundamentals and Applications*, edited by H. E. Bergna and W. O. Roberts (Taylor and Francis, 2006) pp. 247–252.